JOURNAL OF GUIDANCE, CONTROL, AND DYNAMICS
Vol. 32, No. 2, March–April 2009

Optimal Design of Satellite Formation Relative Motion Orbits Using Least-Squares Methods

Hui Yan,* Kyle T. Alfriend,† Srinivas R. Vadali,‡ and Prasenjit Sengupta§
Texas A&M University, College Station, Texas 77843-3141

DOI: 10.2514/1.35044

Formation flying relative orbit design can be achieved by determining six initial conditions in the local-vertical–local-horizontal frame or, equivalently, six differential orbital elements. In this paper, two novel approaches are proposed to design perturbed satellite formation relative motion orbits using least-squares techniques. First, it is shown that the initial conditions required to approximate a desired formation geometry can be analytically solved for by using the Gim–Alfriend state transition matrix in conjunction with a linear least-squares approach. An improvement to this method is obtained by using the Gaussian least-squares differential correction approach and numerical integration of the equations of motion of the two satellites. Numerical results are presented to demonstrate the applications of the two approaches.

I. Introduction

SATELLITE formation flying has received much attention for terrestrial observation, communication, and stellar interferometry in recent years, due to the advantages of flexibility and low cost. Because the analysis of perturbed relative motion of satellites is very complicated, much effort has been devoted to the simplification of relative motion dynamic models for the design and propagation of relative orbits. The first published study in the United States on the relative motion of close or neighboring satellites was performed by Clohessy and Wiltshire [1], hence the often used name, the Clohessy–Wiltshire (C-W) equations. These equations assume that motion is about a spherical Earth, the reference orbit is circular, and the distance between the satellites is small compared to the orbit radius, a basis for linearizing the equations of motion.

Tschauner and Hempel [2] and Lawden [3] derived the relative motion equations for eccentric orbits. Satellite formation design can be accomplished by selecting six initial conditions for relative motion in the local-vertical–local-horizontal (LVLH) frame or, equivalently, the six differential orbital elements. Inalhan et al. [4] and Sengupta et al. [5] considered the effects of the reference orbit eccentricity on the relative motion initial conditions. Gim and Alfriend [6] obtained the state transition matrix (STM) for relative motion including the effects of eccentricity and gravity perturbation J_2. Several approximate theories of relative motion were compared by Alfriend and Yan [7].

Sabol et al. [8] investigated the effect of gravitational perturbations and atmospheric drag on satellite formation designs based on the solutions of the C-W equations. Alfriend et al. [9] have obtained the linear relationship between relative motion in the LVLH frame and differential orbital elements to account for the effects of eccentricity and gravity perturbation J_2. This feature has also been used by Vadali et al. [10], Alfriend and Yan [7], and Schaub [11] to design formations in noncircular orbits. A zero-secular along-track drift condition is used to determine the differential semimajor axis in [10]. The characterization of the relative orbit geometry is achieved by relating the rest of the orbital element differences to its shape, size, and the initial phase angle. Sengupta and Vadali [12] and Lane and Axelrad [13] parameterize relative motion in terms of integration constants and differential orbital elements to design relative motion orbits for eccentric reference orbits, but J_2 is not incorporated into the equations.

In this paper, two novel approaches are proposed to design satellite formation relative orbits using least-squares techniques. First, it is shown that the initial conditions required to approximate the desired formation geometry can be analytically solved for by using the Gim–Alfriend state transition matrix in conjunction with a linear least-squares approach. In this approach, the errors between the STM-predicted relative orbit solutions at a number of points in time and the corresponding reference values from the C-W equations are minimized in a least-squares sense to obtain the optimal design. The Gaussian least-squares differential correction (GLSDC) approach improves upon the simpler linear least-squares method by using the nonlinear equations of motion of the two satellites. This approach is similar to the standard method of orbit determination using GLSDC [14], the only difference being that the measurements are given by the reference or desired relative orbit geometry. The GLSDC procedure can be used for designing relative orbits that are not necessarily small in size. Several numerical results are included to demonstrate the applications of the two approaches.

II. Desired Formation Flying Relative Orbit

We use a projected circular orbit (PCO) as an example. A PCO is an elliptic relative orbit but, as the name implies, it has a circular projection in the local horizontal plane. In a chief centered LVLH frame $oxyz$, a PCO can be described by

$$x(t) = k_1 \sin(nt + \alpha_0) \tag{1}$$

$$y(t) = 2k_1 \cos(nt + \alpha_0) \tag{2}$$

$$z(t) = k_2 \sin(nt + \alpha_0) \tag{3}$$

$$\dot{x}(t) = k_1 n \cos(nt + \alpha_0) \tag{4}$$

$$\dot{y}(t) = -2k_1 n \sin(nt + \alpha_0) \tag{5}$$

$$\dot{z}(t) = k_2 n \cos(nt + \alpha_0) \tag{6}$$

Presented at the 17th AAS/AIAA Space Flight Mechanics Conference, Sedona, AZ, 28 January–1 February 2007; received 8 October 2007; revision received 17 December 2008; accepted for publication 19 December 2008.

*Postdoctoral Associate, Department of Aerospace Engineering; hyan@tamu.edu. Senior Member AIAA.

†Texas Engineering Experiment Station Distinguished Research Chair Professor, Department of Aerospace Engineering; alfriend@aero.tamu.edu. Fellow AIAA.

‡Stewart & Stevenson Professor, Department of Aerospace Engineering; svadali@aero.tamu.edu. Associate Fellow AIAA.

§Postdoctoral Associate, Department of Aerospace Engineering; prasenjit@tamu.edu. Member AIAA.

where

$$2k_1 = k_2 = \rho \tag{7}$$

In the preceding equations, ρ is the relative orbit size and α_0 is the in-plane phase angle. The initial phase angle is defined, at the time of equator crossing of the chief, in the local horizon oyz plane, as shown in Fig. 1.

Note that x, y, and z are the LVLH Cartesian coordinates, and $\dot{x}$, $\dot{y}$, and $\dot{z}$ are the relative velocity components in this frame. The mean motion n is given by $n = \sqrt{\mu/a^3}$, where μ is the gravitational parameter, a is the semimajor axis, and t is time.

A geometrical method [7,10,12,15] involving the mean orbital elements has been widely used to design relative orbits. To avoid the singularity for small eccentricities associated with the classical elements, a set of nonsingular orbital elements is used in [12]

$$e = [a, \lambda, i, q_1, q_2, \Omega] \tag{8}$$

$$q_1 = e\cos\omega \tag{9}$$

$$q_2 = e\sin\omega \tag{10}$$

where e is the eccentricity, i is the inclination, Ω is the longitude of ascending node, ω is the argument of perigee, and λ is the mean argument of latitude. The differential orbital elements are determined from the selected relative motion orbit. They are [12]

$$\delta i = \frac{\rho_3}{p}\cos\beta_0 \tag{11}$$

$$\delta\Omega = -\frac{\rho_3}{p}\frac{\sin\beta_0}{\sin i} \tag{12}$$

$$\delta q_1 = q_1 q_2 \frac{\rho_1}{p}\cos\alpha_0 - (1 - q_1^2)\frac{\rho_1}{p}\sin\alpha_0 - q_2\left(\frac{\rho_2}{p} - \delta\Omega\cos i\right) \tag{13}$$

$$\delta q_2 = q_1 q_2 \frac{\rho_1}{p}\sin\alpha_0 - (1 - q_2^2)\frac{\rho_1}{p}\cos\alpha_0 + q_1\left(\frac{\rho_2}{p} - \delta\Omega\cos i\right) \tag{14}$$

$$\delta\lambda = \left(\frac{\rho_2}{p} - \delta\Omega\cos i\right) - \frac{(1 + \eta + \eta^2)}{(1 + \eta)}\frac{\rho_1}{p}(q_1\cos\alpha_0 - q_2\sin\alpha_0) \tag{15}$$

where p is the semiparameter, ρ_1 and ρ_3 are the size parameters (in-plane and out-of-plane, respectively), ρ_2 is the along-track bias, β_0 is the out-of-plane phase angle, and $\eta = \sqrt{1 - e^2}$. The sixth initial condition, on the differential semimajor axis, is obtained in terms of nonsingular elements from the result of [10]

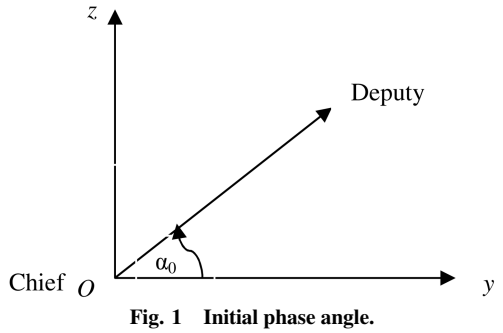

Fig. 1 Initial phase angle.

$$\delta a = -0.5 J_2 a\left(\frac{R_e}{a}\right)^2\left(\frac{3\eta + 4}{\eta^4}\right) \times\left[(1 - 3\cos^2 i)\left(\frac{q_1\delta q_1 + q_2\delta q_2}{\eta^2}\right) + \sin 2i\delta i\right] \tag{16}$$

where J_2 is the gravitational perturbation and R_e is the Earth radius.

III. Formation Design Using Linear Least Squares

The geometrical method uses a mapping between the orbital element differences and the shape and size parameters of the desired formation. The differential orbital elements are used to obtain the initial conditions of the deputy, given the same for the chief. Here, we use a least-squares method to set up the desired formation flying relative orbit, that is., determine the initial conditions for the relative orbit numerically. Because PCO solutions are based on the C-W equations, the least-squares method is very suitable for minimizing the perturbations from J_2, eccentricity, nonlinearity, and other effects as well.

The desired values of the relative motion states at the sample points t_i, $i = 0, 1, 2, \ldots, m$, are obtained from Eqs. (1–6) and are arranged as follows:

$$\tilde{\mathbf{y}} = \mathbf{x}_r = [\mathbf{x}_{r0}^T, \mathbf{x}_{r1}^T, \ldots, \mathbf{x}_{rm}^T]^T \tag{17}$$

where $\mathbf{x} = [x, \dot{x}, y, \dot{y}, z, \dot{z}]^T$ and the subscript r is used to denote the reference orbit. Because the reference orbit data of Eq. (17) is obtained from the solution to the C-W equations, it will not fit the J_2 model data exactly, more so for large relative orbits. Thus, the crux of the problem boils down to choosing the best initial condition to minimize the residual error between the outputs of the two models. Let the actual initial condition (hitherto unknown) for the J_2 model be denoted by $\mathbf{x}_0$. Using the Gim–Alfriend STM, we have

$$\mathbf{x}_i = \phi_i(t_i, t_0)\mathbf{x}_0, \qquad i = 0, 1, \ldots, m \tag{18}$$

$$\phi_0 = I \tag{19}$$

where ϕ_i is the STM relating the states at t_i and t_0, and I is an identity matrix.

Define

$$\mathbf{z} = [\mathbf{x}_0^T, \mathbf{x}_1^T, \ldots, \mathbf{x}_m^T]^T \tag{20}$$

$$\mathbf{z} = \Phi\mathbf{x}_0 \tag{21}$$

where $\Phi = [\phi_0^T, \phi_1^T, \ldots, \phi_m^T]^T$. Then, the optimal choice for the initial conditions $\mathbf{x}_0$ that minimizes the sum of the squared errors between the actual and reference values

$$J = \tfrac{1}{2}(\tilde{\mathbf{y}} - \mathbf{z})^T W(\tilde{\mathbf{y}} - \mathbf{z}) = \tfrac{1}{2}(\tilde{\mathbf{y}} - \Phi\mathbf{x}_0)^T W(\tilde{\mathbf{y}} - \Phi\mathbf{x}_0) \tag{22}$$

is given by

$$\mathbf{x}_0 = (\Phi^T W\Phi)^{-1}\Phi^T W\mathbf{x}_r \tag{23}$$

where W is a weighting matrix used to weight the relative importance of each element. The preceding linear least-squares approach has limited applicability due to the local linear approximation employed. A more general approach for determining the best fit J_2-perturbed relative orbit close to a desired C-W orbit is discussed in the following section.

IV. Formation Flying Design Using Gaussian Least-Squares Differential Correction

GLSDC was discovered by Gauss as a method to solve a complete orbit determination problem. This algorithm is the most commonly applied nonlinear estimation method. Given the initial conditions of the chief, it is a nontrivial task to determine the initial conditions of the deputy to generate the desired formation flying relative orbits. In

fact, the initial conditions may not exist for a closed relative orbit under general perturbations. Here, we consider as the perfect measurements $\tilde{\mathbf{y}}$, the desired formation state as given by Eq. (17) and use GLSDC to estimate the relative motion initial conditions to make the generated relative orbits to be as close to the desired orbit as possible.

The GLSDC finds an estimate $\hat{\mathbf{x}}_0$ for $\mathbf{x}_0$ that minimizes the cost function

$$J = \tfrac{1}{2}[\tilde{\mathbf{y}} - \mathbf{h}(\hat{\mathbf{x}}_0)]^T W[\tilde{\mathbf{y}} - \mathbf{h}(\hat{\mathbf{x}}_0)] \tag{24}$$

where $\mathbf{h}(\hat{\mathbf{x}}_0)$ is an estimated output function of the estimated initial condition $\hat{\mathbf{x}}_0$. In the problem of interest, $\mathbf{h}(\hat{\mathbf{x}}_0)$ is a vector consisting of the states of the relative orbit at time points t_i, $i = 0, 1, 2, \ldots, m$, obtained from numerical integration of the equations of motion of the chief and deputy. The guessed or estimated initial relative state $\hat{\mathbf{x}}_0$ is used to obtain the initial conditions of the deputy in the Earth-centered inertial frame. A correction to the estimate of $\mathbf{x}_0$ at the ith iteration $\hat{\mathbf{x}}_{0,i}$ is

$$\Delta\hat{\mathbf{x}}_{0,i} = (H^T W H)^{-1} H^T W \Delta\mathbf{y}_i \tag{25}$$

where

$$\Delta\mathbf{y}_i \equiv \tilde{\mathbf{y}} - \mathbf{h}(\hat{\mathbf{x}}_{0,i}) \tag{26}$$

and

$$H = \frac{\partial \mathbf{h}}{\partial \mathbf{x}}\Big|_{\mathbf{x}_{0,i}}$$

is the Jacobian matrix. The updated equation is

$$\hat{\mathbf{x}}_{0,i+1} = \hat{\mathbf{x}}_{0,i} + \Delta\hat{\mathbf{x}}_{0,i} \tag{27}$$

Figure 2 shows the complete GLSDC algorithm for formation design. In Fig. 2, we assume that the orbital elements of the chief are known. First, we guess the initial relative state $\hat{\mathbf{x}}_\mathbf{0}$, from which the Cartesian initial conditions of the deputy's orbit can be determined. We then use the initial conditions of the chief and deputy to integrate Eqs. (28–33) for each satellite in the inertial frame:

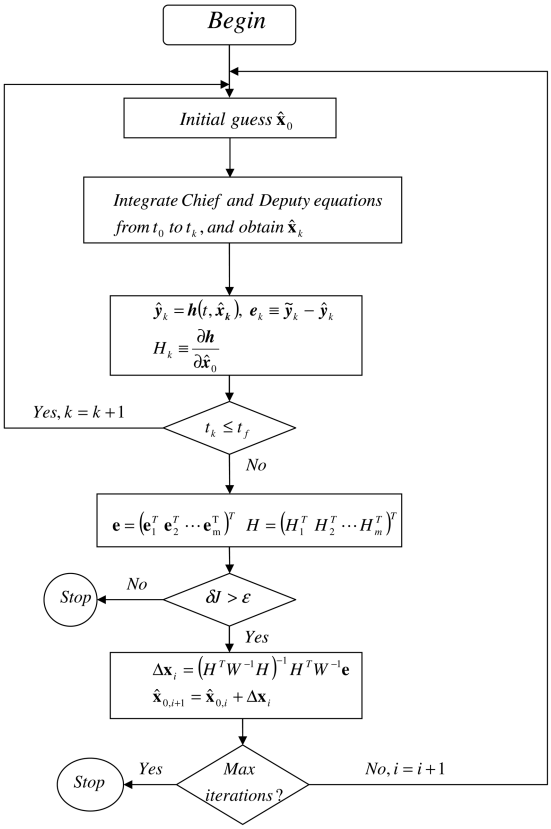

Fig. 2 Optimal nonlinear relative orbit design.

$$\dot{X} = V_X \tag{28}$$

$$\dot{Y} = V_Y \tag{29}$$

$$\dot{Z} = V_Z \tag{30}$$

$$\ddot{X} = -\frac{\mu X}{r^3}\left[1 - \frac{3}{2}J_2\left(\frac{R_e}{r}\right)^2\left(5\frac{Z^2}{r^2} - 1\right)\right] + u_X \tag{31}$$

$$\ddot{Y} = -\frac{\mu Y}{r^3}\left[1 - \frac{3}{2}J_2\left(\frac{R_e}{r}\right)^2\left(5\frac{Z^2}{r^2} - 1\right)\right] + u_Y \tag{32}$$

$$\ddot{Z} = -\frac{\mu Z}{r^3}\left[1 - \frac{3}{2}J_2\left(\frac{R_e}{r}\right)^2\left(5\frac{Z^2}{r^2} - 3\right)\right] + u_Z \tag{33}$$

where X, Y, and Z are the coordinates in the inertial frame, and $r = \sqrt{X^2 + Y^2 + Z^2}$. The inertial frame is defined such that the X axis points to the vernal point in the equatorial plane of the Earth, the Z axis is the axis of rotation of the Earth in a positive direction, and Y is defined by the right-hand rule. For the investigation reported in this paper, we assume no control acceleration, that is, $u_X = u_Y = u_Z = 0$. Next, we use Eqs. (34–39) to obtain the relative states $\mathbf{x}$ [10]:

$$x = \frac{\delta\mathbf{r}^T\mathbf{r}_c}{r_c} \tag{34}$$

$$y = \frac{\delta\mathbf{r}^T(\mathbf{H_c} \times \mathbf{r}_c)}{|\mathbf{H_c} \times \mathbf{r}_c|} \tag{35}$$

$$z = \frac{\delta\mathbf{r}^T\mathbf{H}_c}{H_c} \tag{36}$$

$$\dot{x} = \frac{\delta\mathbf{v}^T\mathbf{r}_c + \delta\mathbf{r}^T\mathbf{v}_c}{r_c} - \frac{(\delta\mathbf{r}^T\mathbf{r}_c)(\mathbf{r}_c^T\mathbf{v}_c)}{r_c^3} \tag{37}$$

$$\dot{y} = \frac{\delta\mathbf{v}^T(\mathbf{H}_c \times \mathbf{r}_c) + \delta\mathbf{r}^T(\dot{\mathbf{H}}_c \times \mathbf{r}_c + \mathbf{H}_c \times \mathbf{v}_c)}{|\mathbf{H}_c \times \mathbf{r}_c|} - \frac{\delta\mathbf{r}^T(\mathbf{H}_c \times \mathbf{r}_c)(\mathbf{H}_c \times \mathbf{r}_c)^T(\dot{\mathbf{H}}_c \times \mathbf{r}_c + \mathbf{H}_c \times \mathbf{v}_c)}{|\mathbf{H}_c \times \mathbf{r}_c|^3} \tag{38}$$

$$\dot{z} = \frac{\delta\mathbf{v}^T\mathbf{H}_c + \delta\mathbf{r}^T\dot{\mathbf{H}}_c}{H_c} - \frac{\delta\mathbf{r}^T\mathbf{H}_c(\mathbf{H}_c^T\dot{\mathbf{H}}_\mathbf{c})}{H_c^3} \tag{39}$$

where $\delta\mathbf{r}$ and $\delta\mathbf{v}$ are, respectively, the relative position and velocity vectors expressed in the inertial frame, and $\mathbf{H} = \mathbf{r} \times \mathbf{v}$ is the angular momentum vector. The subscript c is used to denote the chief.

The Jacobian matrix is

$$H_k = \frac{\partial \mathbf{h}}{\partial \hat{\mathbf{x}}_0} = \frac{\partial \mathbf{h}}{\partial \hat{\mathbf{x}}_k}\frac{\partial \hat{\mathbf{x}}_k}{\partial \hat{\mathbf{x}}_0} = \frac{\partial \mathbf{h}}{\partial \hat{\mathbf{x}}_k}\phi_k(t_k, t_0) \tag{40}$$

where $\phi_k(t_k, t_0)$ is the state transition matrix. The convergence function is

$$\delta J = \left|\frac{J_{i+1} - J_i}{J_{i+1}}\right| \le \varepsilon \tag{41}$$

where ε is a tolerance parameter.

V. Gim–Alfriend State Transition Matrix

The state transition matrix developed by Gim and Alfriend [6] can be written using the following notation:

$$\mathbf{x}(t) = \{\mathbf{a}(t) + \alpha\mathbf{b}(t)\}\delta\mathbf{e} \tag{42}$$

$$\mathbf{x}(t) = \phi(t, t_0)\mathbf{x}(t_0) \tag{43}$$

where $\delta\mathbf{e}$ is the differential orbital element vector and the STM is

$$\phi(t, t_0) = \{\mathbf{A}(t) + \xi\mathbf{B}(t)\}\mathbf{D}(t)\bar{\phi}_e(t, t_0)\mathbf{D}^{-1}(t_0)\{\mathbf{A}(t) + \xi\mathbf{B}(t)\}^{-1} \tag{44}$$

where $\xi = 3J_2R_e^2$. The matrix $\mathbf{B}(t)$ contains only the terms due to J_2, the STM for the relative mean elements is $\bar{\phi}_e(t)$, and $\mathbf{D}(t)$ is the Jacobian of the mean to osculating element transformation.

VI. Numerical Results

The nonsingular mean elements of the chief's orbit selected in this paper are

$$a = 8000 \text{ km}, \qquad \lambda = 0, \qquad i = 50 \text{ deg}$$
$$q_1 = 0.01, \qquad q_2 = 0, \qquad \Omega = 0 \text{ deg}$$

The following sections present the results obtained by using the two methods discussed earlier.

A. Formation Design Using Linear Least Squares

The number of the evenly spaced sampling points are selected to be $m = 500$ over 10 orbital periods. The required geometric parameters are chosen as $\alpha_0 = 0$ and $\rho = 100$ km. The weighting matrix $\mathbf{W}$ in Eq. (24) is

$$[\mathbf{W}]_{ij} = \begin{cases} \mathbf{O} & i \neq j \\ \mathbf{R} & i = j \end{cases} i, \quad j = 0, 1, 2, \ldots, m \tag{45}$$

where $\mathbf{O}$ is the 6×6 zero matrix and $\mathbf{R}$ is the 6×6 scaling matrix

$$\mathbf{R} = \text{diag}(1/R_e^2, R_e/\mu, 1/R_e^2, R_e/\mu, 1/R_e^2, R_e/\mu) \tag{46}$$

The matrix $\mathbf{R}$ is selected in terms of the Earth-value units so that the cost function can be evaluated in canonical units.

The initial conditions resulting from Eq. (23) are

$$\mathbf{x}_0 = [-2.63\text{e}-1, 4.49\text{e}-2, 9.96\text{e}1, 4.12\text{e}-4, -1.90\text{e}-1, 8.91\text{e}-2]^T \tag{47}$$

The units are kilometers and kilometers per second for position and velocity, respectively. Table 1 lists the mean nonsingular elements obtained using two different procedures.

In Table 1, IC1 indicates the mean differential nonsingular elements obtained by using the inverse transformation of Eq. (42) with the initial conditions $\mathbf{x}_0$ from Eq. (23) and the transformation from the osculating to mean nonsingular elements. The initial conditions calculated from Eqs. (11–16) by using the geometrical method are represented by IC2. As can be seen, the initial conditions obtained from the least-squares method agree very well with those from the geometrical method. Also, the validity of the period-matching condition in Eq. (16) is verified by the linear least-squares technique, because the differential semimajor axis results from the two approaches match very well. The results of simulating relative motion by using the two sets of the initial conditions are shown next.

The simulation time is 50 orbital periods. Note that the time span used for the least-squares procedure is 10 orbits, so the simulation is 40 orbits beyond the least-squares fit span. Figure 3 shows the errors in the orbit radius due to the least-squares and geometrical method. The maximum error is about 3% of that of the reference PCO.

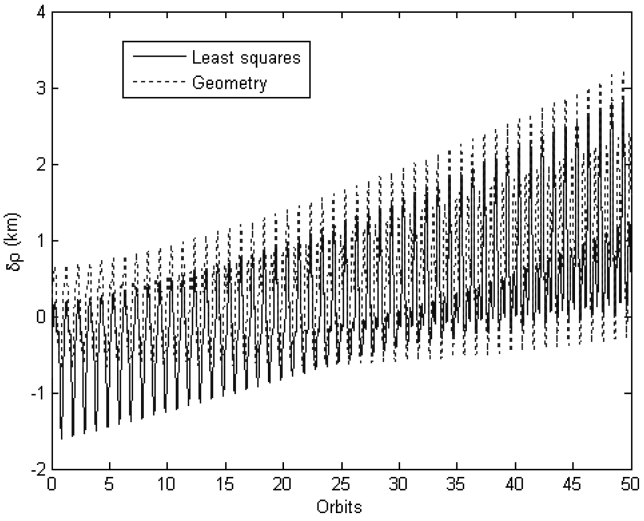

Fig. 3 Evolution of the error in the radius of the PCO.

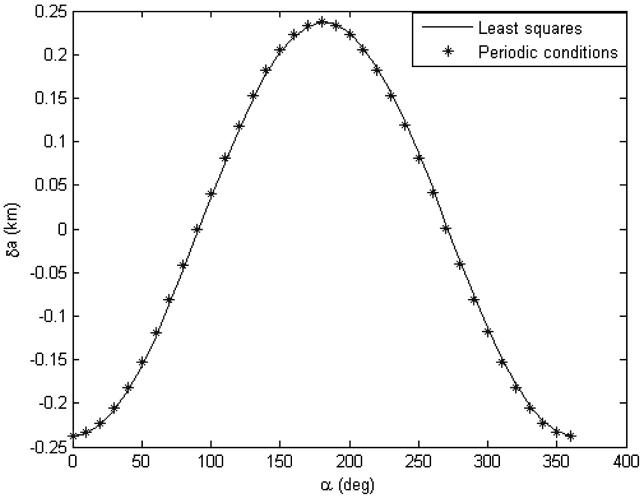

Fig. 4 Period matching condition verification.

The validity of the period-matching condition is further verified by varying the initial phase angle, as shown in Fig. 4. Data in Fig. 4 are obtained for initial phase angles separated by 10 deg, using both the least-squares method and the first-order period-matching condition of Eq. (16).

Figure 5 evaluates the effect of the least-squares fit span on δa and compares this result to that obtained from Eq. (16). The two methods are in excellent agreement except for a fit span of less than one orbit. The period-matching condition is independent of the fit span, so its result is constant. The least-squares method is finding the δa that will minimize the error between the actual and desired PCO. The desired PCO is based on a circular orbit, but the actual orbit is eccentric. Therefore, in addition to the secular in-track error resulting, there is a periodic error due to the eccentricity. For a fit span of less than one orbit, this periodic error can be significant when compared to the secular error. As a result, δa obtained from the least-squares procedure is varying as it tries to compensate for this eccentricity effect. As the fit span increases, the secular error dominates and the two approaches agree. (After one orbit, the fit span was chosen to be integer orbits and the in-track eccentricity error is zero here. If

Table 1 Comparison for the initial conditions of the radius 100 km

	δa, km	$\Delta\lambda$, rad	δi, rad	δq_1	δq_2	$\delta\Omega$, rad
IC1	$-2.369\text{e}-1$	$-1.487\text{e}-4$	1.250e-2	2.460e-5	$-6.240\text{e}-3$	3.685e-5
IC2	$-2.372\text{e}-1$	$-9.376\text{e}-5$	1.250e-2	0	$-6.251\text{e}-3$	0

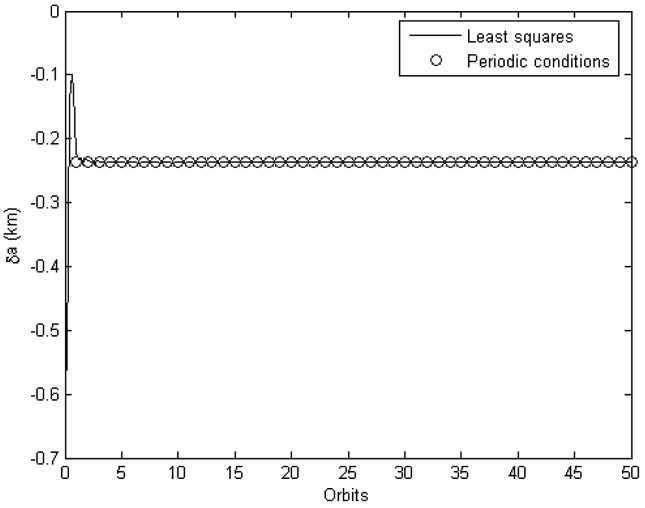

Fig. 5 Variation of δa with time.

computed at smaller intervals, the least-squares curve would oscillate and asymptotically approach that for the period-matching condition orbit.) Furthermore, Figs. 4 and 5 reveal that the period-matching condition provides a good basis for the optimal design of moderately large formations.

B. Formation Design Using Gaussian Least-Squares Differential Correction

This section presents the results obtained from the GLSDC method. The radius of the relative orbit is 100 km. The convergence of the method has been tested by using three sets of initial guesses. The first initial guess is obtained from the transformation of the differential orbital elements of Eqs. (11–16) into a relative initial state vector. The second initial guess is provided directly by Eqs. (1–6), evaluated at $t = 0$. The third initial guess is arbitrarily chosen: $x_0 = y_0 = z_0 = 1$ km and $\dot{x}_0 = \dot{y}_0 = \dot{z}_0 = 0.001$ km/s. The number of sample points for all the test cases is 500 and the initial conditions are determined based on a fit span of 10 orbits. The convergence parameter is set as $\varepsilon = 1\mathrm{e} - 8$. Our results show that the GLSDC converges for each initial guess to the same estimate of the initial state vector. The convergence is very fast and the number of the iterations is less than 10 for each initial guess. The best fit relative orbit is shown in Fig. 6 and the stars represent the reference values.

Figure 6 indicates that the relative orbit from the solutions of GLSDC matches the desired PCO extremely well. To illustrate the difference between the GLSDC and linear least-squares methods, Fig. 7 shows the effect of the periodic matching conditions as a function of the radius of the relative orbit using the geometrical method, linear least squares, and GLSDC.

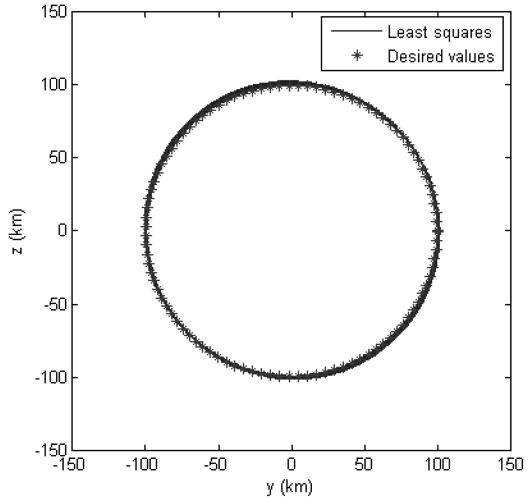

Fig. 6 Relative orbit iterated from GLSDC.

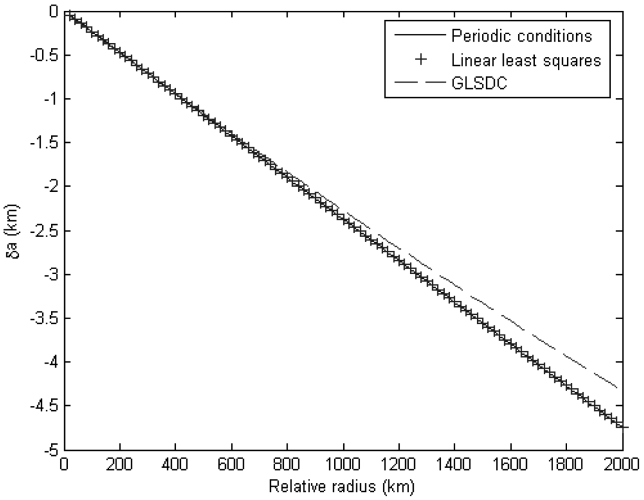

Fig. 7 Comparison for periodic matching conditions.

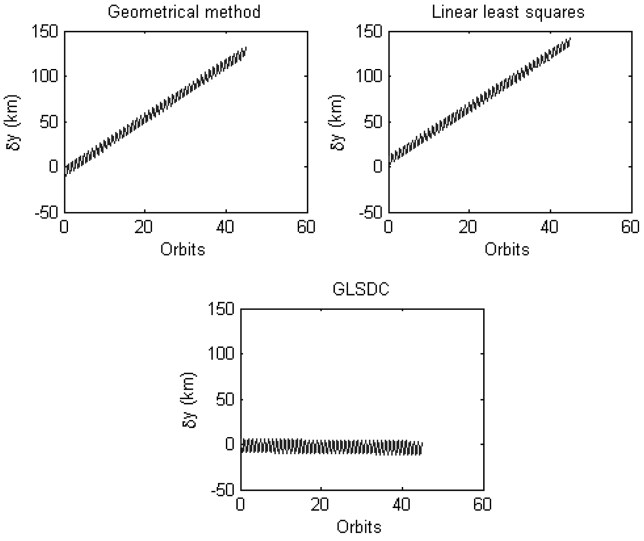

Fig. 8 Error growth comparisons in the in-track direction.

In Fig. 7, the solid line presents the variation of δa with ρ as obtained from Eq. (16), whereas the plus signs and dashed lines stand for the solutions from the linear least squares and GLSDC, respectively. The results obtained from the linear least squares agree very well with those from the geometrical method, and indicate that δa is a linear function of the size of relative orbit. The effects of nonlinearity can be seen for orbit radii greater than 600 km. The ability of GLSDC to account for nonlinearities and keep the along-track motion bounded for very large relative motion orbits is shown in Fig. 8 for a relative orbit radius of 2000 km. Note that out-of-plane motion cannot be kept bounded without the use of control. Along-track error growths shown for the three methods for a period of 50 orbits indicate the effectiveness of the GLSDC method.

The δa calculated by the geometrical method, linear least squares, and GLSDC are -4.7395, -4.7379, and -4.3603 km, respectively.

VII. Conclusions

This paper has shown that least-squares techniques can be used to design desired satellite formation relative orbits subject to perturbations. Initial conditions required to best fit the desired formation geometry can be analytically solved for by using the Gim–Alfriend state transition matrix in conjunction with a linear least-squares approach. An improvement to the linear least-squares

method is obtained by using the Gaussian least-squares differential correction procedure and numerical integration of the equations of motion of the two satellites. GLSDC performs better than the linear least-squares approach, especially for relative orbits that are larger than 100 km in size. Unlike the geometrical method developed for a specific gravitational perturbation model, the linear and nonlinear least-squares methods can handle more general perturbations. The least-squares methods are not limited to formation flying orbit design, they can also be applied to other trajectory designs to optimally accommodate a class of perturbations without incurring fuel expenditure to cancel their effects.

References

[1] Clohessy, W. H., and Wiltshire, R. S., "Terminal Guidance System for Satellite Rendezvous," *Journal of the Astronautical Sciences*, Vol. 27, No. 9, Sept. 1960, pp. 653–678.

[2] Tschauner, J., and Hempel, P., "Optimale Beschleunigeungsprogramme fur das Rendezvous-Manover," *Astronautica Acta*, Vol. 10, Nos. 5–6, 1964, pp. 296–307.

[3] Lawden, D. F., *Optimal Trajectories for Space Navigation*, Butterworths, London, 1963.

[4] Inalhan, G., Tillerson, M., and How, J. P., "Relative Dynamics and Control of Spacecraft Formations in Eccentric Orbits," *Journal of Guidance, Control, and Dynamics*, Vol. 25, No. 1, Jan.–Feb. 2002, pp. 48–59.
doi:10.2514/2.4874

[5] Sengupta, P., Sharma, R., and Vadali, S. R., "Periodic Relative Motion Near a Keplerian Elliptic Orbit with Nonlinear Differential Gravity," *Journal of Guidance, Control, and Dynamics*, Vol. 29, No. 5, 2006, pp. 1110–1121.
doi:10.2514/1.18344

[6] Gim, D.-W., and Alfriend, K. T., "State Transition Matrix of Relative Motion for the Perturbed Noncircular Reference Orbit," *Journal of Guidance, Control, and Dynamics*, Vol. 26, No. 6, Nov.–Dec. 2003, pp. 956–971.
doi:10.2514/2.6924

[7] Alfriend, K. T., and Yan, H., "An Evaluation and Comparison of Relative Motion Theories," *Journal of Guidance, Control, and Dynamics*, Vol. 28, No. 2, 2005, pp. 254–261.
doi:10.2514/1.6691

[8] Sabol, C., Burns, R., and McLaughlin, C. A., "Satellite Formation Flying Design and Evolution," *Journal of Spacecraft and Rockets*, Vol. 38, No. 2, 2001, pp. 270–278.
doi:10.2514/2.3681

[9] Alfriend, K. T., Schaub, H., and Gim, D.-W., "Gravitational Perturbations, Nonlinearity and Circular Orbit Assumption Effect on Formation Flying Control Strategies," *AAS Guidance and Conference*, American Aeronautical Society Paper 00-012, Feb. 2000.

[10] Vadali, S. R., Vaddi, S. S., and Alfriend, K. T., "An Intelligent Control Concept for Formation Flying Satellites," *International Journal of Robust and Nonlinear Control*, Vol. 12, Nos. 2–3, 2002, pp. 97–115.
doi:10.1002/rnc.678

[11] Schaub, H., "Relative Orbit Geometry Through Classic Orbit Element Differences," *Journal of Guidance, Control, and Dynamics*, Vol. 27, No. 5, 2004, pp. 839–848.
doi:10.2514/1.12595

[12] Sengupta, P., and Vadali, S. R., "Formation Design and Geometry near a Keplerian Orbit with Arbitrary Eccentricity," *Journal of Guidance, Control, and Dynamics*, Vol. 30, No. 4, 2007, pp. 953–964.
doi:10.2514/1.25941

[13] Lane, C., and Axelrad, P., "Formation Design in Eccentric Orbits Using Linearized Equations of Relative Motion," *Journal of Guidance, Control, and Dynamics*, Vol. 29, No. 1, 2006, pp. 146–160.
doi:10.2514/1.13173

[14] Crassidis, J. L., and Junkins, J. L., *Optimal Estimation of Dynamics Systems*, CRC Press, Boca Raton, FL, 2004, pp. 205–213.

[15] Vaddi, S. S., Alfriend, K. T., Vadali, S. R., and Sengupta, P., "Formation Establishment and Reconfiguration Using Impulsive Control," *Journal of Guidance, Control, and Dynamics*, Vol. 28, No. 2, 2005, pp. 262–268.
doi:10.2514/1.6687